

Ab Initio QM/MM Simulation of Ag⁺ in 18.6% Aqueous Ammonia Solution: Structure and Dynamics Investigations

Ria Armunanto,[†] Christian F. Schwenk, and Bernd M. Rode*

Department of Theoretical Chemistry, Institute of General, Inorganic, and Theoretical Chemistry, University of Innsbruck, Innrain 52a, A-6020 Innsbruck, Austria

Received: August 17, 2004; In Final Form: February 21, 2005

Structure and dynamics investigations of Ag⁺ in 18.6% aqueous ammonia solution have been carried out by means of the ab initio quantum mechanical/molecular mechanical (QM/MM) molecular dynamics (MD) simulation method. The most important region, the first solvation shell, was treated by ab initio quantum mechanics at the Restricted Hartree–Fock (RHF) level using double- ζ plus polarization basis sets for ammonia and plus ECP for Ag⁺. For the remaining region in the system, newly constructed three-body corrected potential functions were used. The average composition of the first solvation shell was found to be [Ag(NH₃)₂(H₂O)_{2.8}]⁺. No ammonia exchange process was observed for the first solvation shell, whereas ligand exchange processes occurred with a very short mean residence time of 1.1 ps for the water ligands. No distinct second solvation shell was observed in this simulation.

1. Introduction

Structure and dynamics information of ionic solvation in multicomponent liquid mixtures is fundamental to understanding the role of ions in biological and chemical systems with different coordination sites. As the Ag⁺ ion and its complexes play an important role in several biological and medical aspects, e.g., as antiethylene and with their antibacterial and antifungal activities,^{1–4} Ag⁺ in aqueous ammonia solution is an interesting model system of high relevance. Several experimental investigations have been carried out with Ag⁺ in aqueous or pure ammonia, yielding varying coordination numbers.⁵ A linear two-coordinated Ag(NH₃)₂⁺ complex was obtained from X-ray diffraction in solid phase⁶ and in aqueous ammonia.⁷ In ammoniacal solutions, different species with coordination numbers between 2 and 4 were found depending on the molar ratio of the ammonia ligands to Ag⁺.⁸ A four-coordinated tetrahedral structure with Ag–N distance of 2.31 Å was observed for 0.2 M solution of AgNO₃ in liquid ammonia using the EXAFS method.⁹ Quantum mechanical/molecular mechanical (QM/MM) simulations of Ag⁺ in water and in liquid ammonia reported a flexible mainly five-coordinated water complex¹⁰ and a stable tetrahedral structure in ammonia,¹¹ respectively. Recent density-functional theory (DFT) calculations of gas-phase complexes of silver with ammonia and/or aquoligands have shown very specific solvation effects of this system.¹⁸

In the present work, the QM/MM molecular dynamics (MD) simulation method, well-known as a powerful tool of theoretical chemistry, is used to investigate structure and dynamics of solvated Ag⁺ in 18.6% aqueous ammonia solution. This method has proven successful in the description of metal–ion solvation in aqueous ammonia solution.^{12–16} Because of the inadequacy of pair potentials to describe interactions nearby the ion, three-

body correction functions were constructed and used for the MM part of the QM/MM simulation. Higher N-body terms as included in the QM region can be neglected in the MM region because of their small contributions to total interactions.

The ion–ligand stretching frequencies, mean residence times, and the lability of the solvation shells as well as structural properties were evaluated, as these fundamental parameters help to understand the reactivity of the ion in the relevant systems. These structural and dynamical properties are very sensitive to the accuracy of the simulation technique, and it has been shown in several cases^{17,19–23} that ab initio QM/MM simulations can reach a sufficient level of accuracy.

2. Methodology

2.1. Construction of Potential Function. To describe MM interactions, a new potential function for H₂O–Ag⁺–NH₃ interactions was constructed; whereas, potential functions for Ag⁺–NH₃,¹¹ Ag⁺–H₂O,¹⁰ NH₃–Ag⁺–NH₃,¹¹ and H₂O–Ag⁺–H₂O¹⁰ interactions were taken from our previous works. The new potential function was developed from ab initio quantum mechanical calculations at the Restricted Hartree–Fock (RHF) level using the Dunning double- ζ plus polarization²⁴ basis set for ammonia and water and the LANL2DZ ECP²⁵ basis set for Ag⁺. Experimental gas-phase values were used for the ammonia (N–H = 1.0124 Å, H–N–H = 106.68°)²⁶ and water (O–H = 0.9601 Å and H–O–H = 104.47°)²⁷ geometries and kept constant throughout the energy calculations. To describe the H₂O–Ag⁺–NH₃ energy surface, more than 8000 ab initio energy points were generated. Three-body correction energies were calculated using the following formula:

$$\Delta E_{\text{corr}}^{3\text{bd}} = (E_{\text{AIW}}^{ab} - E_{\text{I}}^{ab} - E_{\text{A}}^{ab} - E_{\text{W}}^{ab}) - \Delta E_{\text{IA}}^{2\text{bd}}(r_1) - \Delta E_{\text{IW}}^{2\text{bd}}(r_2) - \Delta E_{\text{AW}}^{2\text{bd}}(r_3) \quad (1)$$

where *ab* and 2bd denote ab initio and two-body energies; IA, IW, and AW indicate ion–ammonia, ion–water, and ammonia–water interactions; *r*₁, *r*₂, and *r*₃ correspond to ion–N, ion–O,

* Author to whom correspondence should be addressed: E-mail: bernd.m.rode@uibk.ac.at.

[†] Permanent address: Department of Chemistry, Faculty of Mathematics and Natural Sciences, Austrian-Indonesian Center for Computer Chemistry, Gadjah Mada University, Jogjakarta, Indonesia.

and N–O distances, respectively. These energies were fitted to analytical functions using the Levenberg–Marquardt algorithm. The obtained three-body correction function is:

$$\Delta E_{\text{Fit}}^{\text{3bd}} = 2.60 e^{-0.01(r_1+r_2)} e^{-1.26r_3} (\text{CL} - r_1)^2 (\text{CL} - r_2)^2 \quad (2)$$

where CL, set to 6.0 Å, is the cutoff limit (ion–N and ion–O distances) beyond which three-body terms are negligible.

2.2. Simulation Protocol. The simulations were performed for one Ag⁺, 407 water, and 92 ammonia molecules in a cubic box at 298.16 K, which corresponds to an 18.6% aqueous ammonia solution with the experimental density of 0.927 g/cm³. Periodic boundary conditions were applied to the simulation box, and the temperature was kept constant by the Berendsen algorithm.^{28,29} A flexible ammonia²⁶ and the BJH water³⁰ model, which includes an intramolecular term, were used. The intermolecular potential for the ammonia–water interactions was taken from the literature.¹⁶ Accordingly, the time step of the simulation was set to 0.2 fs, which allows for explicit movement of hydrogens. A cutoff of 12.0 Å was set except for N–Ha, Ha–Ha, and O–Hw and Hw–Hw non-Coulombic interactions for which it was set to 6.0, 5.0, and 5.0 Å and 3.0 Å, respectively (Ha and Hw denote hydrogen atoms of ammonia and water molecules). The reaction field method was used to account for long-range electrostatic interactions.³¹

2.3. QM/MM Molecular Dynamics Simulation. A classical molecular dynamics simulation was carried out for 40.0 ps using the three-body corrected potential functions. Subsequently, the QM/MM simulation was performed for 13 ps after 4 ps of reequilibration. The simulations were performed on two Athlon 1800 XP+ processors, consuming a total simulation time of nearly 200 days. The ab initio HF formalism with the same basis sets used for the construction of the potential was applied to the ion and the full first solvation shell, and for the remaining MM region the same 2 + 3-body potential as in the classical simulation was used. According to the Ag–N and Ag–O RDFs of the classical simulation, the QM radius had to be set to 3.8 Å to include the full first solvation shell. A smoothing function was applied to the transition region between QM and MM regions.²⁸ The force of the system, F_{system} , is defined as:

$$F_{\text{system}} = F_{\text{MM}} + S(F_{\text{QM}} - F_{\text{QM/MM}}) \quad (3)$$

where F_{MM} is the MM force of the full system, F_{QM} the QM force in the QM region, and $F_{\text{QM/MM}}$ the MM force in the QM region. S denotes the smoothing function.³² Free migration of ligands between QM and MM region is enabled in this approach.

2.4. Dynamical Properties Evaluation. The ion–ammonia and ion–water vibrational spectrum were evaluated using velocity autocorrelation functions (VACFs), $C(t)$, defined as:

$$C(t) = \frac{\sum_i^{N_t} \sum_j^N \bar{v}_j(t_i) \bar{v}_j(t_i + t)}{N_t N \sum_i^{N_t} \sum_j^N \bar{v}_j(t_i) \bar{v}_j(t_i)} \quad (4)$$

where N is the number of particles, N_t is the number of time origins t_i , and \bar{v}_j denotes a certain velocity component of particle j . The power spectrum of the VACF was calculated by Fourier transformation. A correlation length of 2.0 ps was used to obtain the power spectra with 2000 (QM/MM) averaged time origins. Ion–ammonia and ion–water vibrational frequencies were then computed using the approximative normal-coordinate analysis.³³

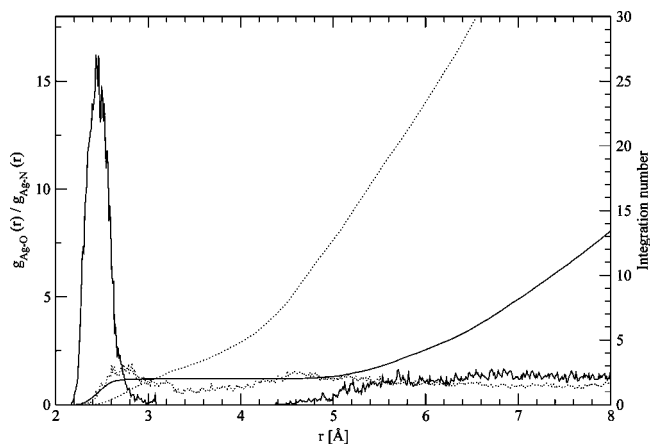


Figure 1. (a) Ag–N (solid line) and (b) Ag–O (dotted line) radial distribution functions and their corresponding integration numbers.

TABLE 1: Characteristic Values of the Radial Distribution Functions $g_{\alpha\beta}(r)$ for Ag⁺ in Liquid Ammonia Obtained from QM/MM MD Simulation^a

α	β	r_M	r_m	$n_{\alpha\beta}(m)$
Ag	N	2.4	3.2	2.0
Ag	O	2.7	3.4	2.8

^a r_M and r_m are the distances in Å of the maxima and minima of $g_{\alpha\beta}(r)$, and $n_{\alpha\beta}(m)$ is the average coordination number integrated up to r_m of the first solvation shell.

The mean residence times (MRTs) of the ligands in the solvation shell of Ag⁺ were calculated by the direct method³⁴ using a t^* value (minimum displacement time for an exchange process to be counted) of 0.5 ps. The lability of the solvation shell can be measured by the sustainability of exchange processes.³⁴ A sustainability coefficient can be defined as:

$$S_{\text{ex}} = \frac{N_{\text{ex}}^{0.5}}{N_{\text{ex}}^0} \quad (5)$$

where N_{ex}^0 is the number of all transitions through a shell boundary, and $N_{\text{ex}}^{0.5}$ means the number of changes persisting after 0.5 picoseconds. The inverse, $1/S_{\text{ex}}$, represents the number of attempts needed to achieve a persistent change of the coordination number.³⁴

3. Results and Discussion

3.1. Structural Data. The radial distribution functions (RDFs) of Ag⁺–N and Ag⁺–O together with their integration numbers obtained from QM/MM MD simulations are displayed in Figure 1, and some characteristic values are listed in Table 1. Well-defined peaks of the Ag⁺–N and Ag⁺–O RDFs define the first and only discrete solvation shell. The sharp peak of the Ag⁺–N RDF located at 2.4 Å indicates a stable Ag(NH₃)₂⁺ complex; whereas, the first broad peak of the Ag⁺–O RDF centered at 2.7 Å represents a labile solvation water structure. The Ag⁺–N distance is slightly lower compared to those obtained from the QM/MM simulation of Ag⁺ in liquid ammonia¹¹ but higher than those of the experimental data^{7,9} (see Table 2). The Ag⁺–O distance is slightly higher in comparison with that obtained from the QM/MM simulation of the ion in pure water¹⁰ but much higher than the EXAFS result.³⁵ The distance discrepancies compared to experimental results are probably caused by the reported instability of the Ag⁺ ion in solution under X-ray irradiation.⁷ Other possible reasons are the extreme lability and asymmetry of the solvation shell of water, leading to the

TABLE 2: Structural Properties of First Solvation Shell of Ag⁺

system	S ^a /cation	d ^b	CN ^c	method	references
Ag ⁺ in aqueous ammonia	499 ^d /1	~2.43 ^{Ag-N}	2.0	QM/MM	this work
Ag ⁺ in liquid ammonia	215/1	~2.74 ^{Ag-O} 2.54 ^{Ag-N}	2.8 4.0	QM/MM	this work ref 11
Ag ⁺ in water	499/1	2.6 ^{Ag-O}	5.4	QM/MM	ref 10
Ag(NH ₃) ₂ NO ₃ solution	14	2.22 ^{Ag-N}	2.0	XRD	ref 7
AgClO ₄ ^e solution	555	2.31 ^{Ag-O}	4.5	EXAFS	ref 35
AgClO ₄ solution	10.5	2.41 ^{Ag-O}	3.9	ND	ref 37

^a S denotes solvent molecule. ^b Distance in Å. ^c Coordination number. ^d Composed by 92 NH₃ and 407 H₂O. ^e In 0.001 M HClO₄.

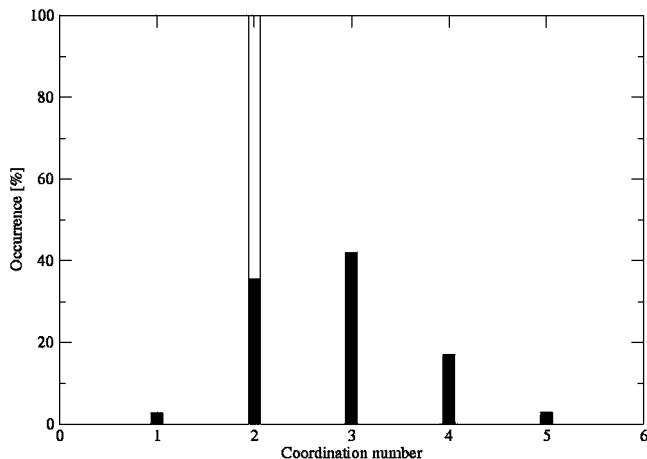


Figure 2. Coordination number distributions of Ag⁺ in 18.6% aqueous ammonia solution: water (dotted bar) and ammonia coordination number distributions obtained from QM/MM MD simulation.

coexistence of more than one configuration within very short time intervals of a few picoseconds. Experimental data averaged over a long time and fitted to a single geometrical model configuration instead of a mixture of geometrically very different configurations might thus lead to somewhat different conclusions. Above ~3.2 Å, the Ag⁺-N RDF remains zero for more than 1 Å, indicating that no ammonia-ligand exchange process take place; whereas, the Ag⁺-O RDF with continuous nonzero value reflects frequent water-ligand exchange processes (vide infra, Figure 6). A second solvation shell is not recognized from either Ag⁺-N or Ag⁺-O RDFs, indicating the influence of the central ion to be too weak to cause a formation of a solvent structure at larger distances.

The coordination number distributions of solvated Ag⁺ are displayed in Figure 2. One hundred percent of 2 for the ammonia coordination number corresponds to a stable Ag(NH₃)₂⁺ complex; whereas, the broad water coordination number distribution indicates that a varying number of water ligands binds to the Ag(NH₃)₂⁺ complex. Experimental data have suggested that in 10 M aqueous ammonia solution, Ag(NH₃)₃⁺ reaches an appreciable concentration. The formation of this complex cannot be excluded because of the short simulation time, but on the other hand, it might be worthwhile to reinvestigate the experimental data interpretation in the light of the varying species distributions found in our study and to investigate possible counterion and Ag⁺ concentration effects.

Five different coordination numbers were observed for water ligands, indicating a very labile water ligand binding to the Ag(NH₃)₂⁺ complex. The 2-, 3- and 4-coordinated water complexes, [Ag(NH₃)₂(H₂O)₂]⁺, [Ag(NH₃)₂(H₂O)₃]⁺, and [Ag(NH₃)₂(H₂O)₄]⁺ dominate. [Ag(NH₃)₂(H₂O)]⁺ and [Ag(NH₃)₂(H₂O)₅]⁺ species are formed in small amounts and can be seen rather as transition state structures. The average coordination number for H₂O molecules in the solvation shell is 2.8. The corresponding H₂O/NH₃ ratio of 1.4 is significantly lower than the whole simulation box (4.4), showing that Ag⁺ strongly

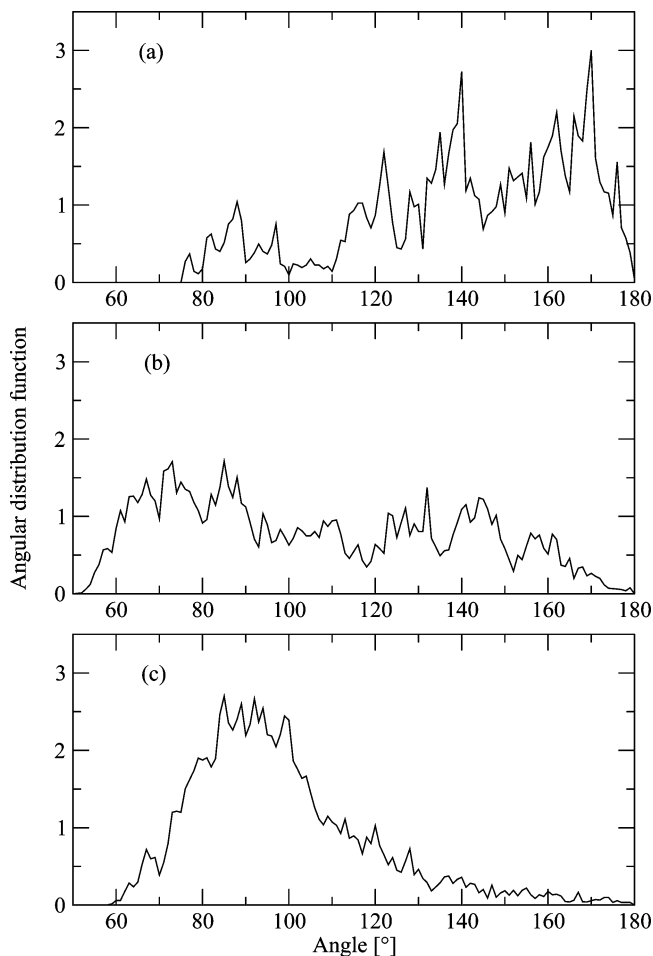


Figure 3. Angular distribution function of (a) N-Ag⁺-N, (b) O-Ag⁺-O, and (c) N-Ag⁺-O angles obtained by QM/MM MD simulations.

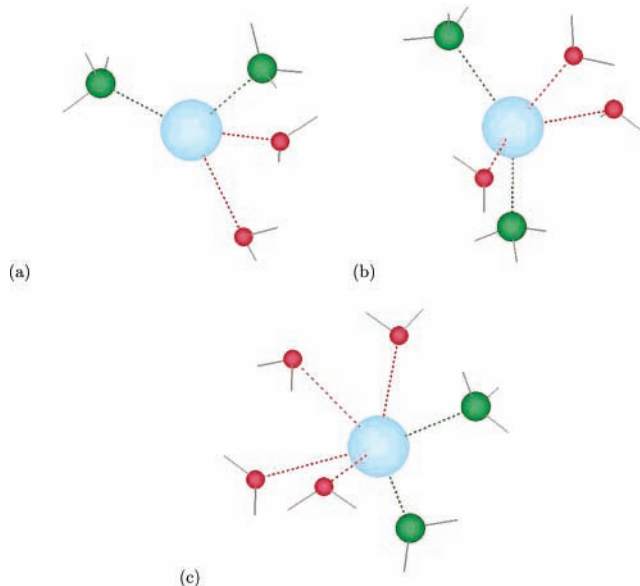


Figure 4. Snapshots of the quantum mechanical region of the QM/MM MD simulation of Ag⁺ in aqueous ammonia, showing three different species coexisting during the simulation.

(H₂O)₅⁺ species are formed in small amounts and can be seen rather as transition state structures. The average coordination number for H₂O molecules in the solvation shell is 2.8. The corresponding H₂O/NH₃ ratio of 1.4 is significantly lower than the whole simulation box (4.4), showing that Ag⁺ strongly

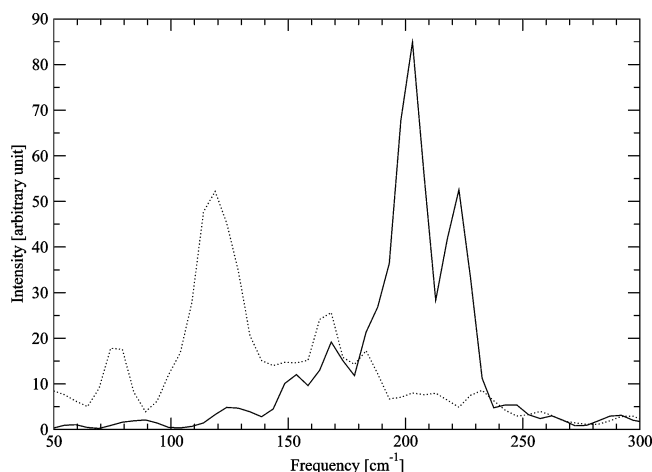


Figure 5. Power spectra of Ag^+ -nitrogen (solid line) and Ag^+ -oxygen vibrational mode in the first solvation shell of Ag^+ in aqueous ammonia solution.

prefers ammonia ligands. Similar results were obtained from our previous QM/MM MD simulations of soft Lewis acids, such as Na^+ and Ca^{2+} ,^{14,15} approving the behavior of the even softer Ag^+ ion.

The $\text{N}-\text{Ag}^+-\text{N}$, $\text{O}-\text{Ag}^+-\text{O}$, and $\text{N}-\text{Ag}^+-\text{O}$ angular distribution functions (ADFs) are depicted in Figure 3. Two peaks located at $\sim 140^\circ$ and $\sim 170^\circ$ were observed for the $\text{N}-\text{Ag}^+-\text{N}$ distribution, indicating that the $\text{Ag}(\text{NH}_3)_2^+$ complex is not always present as a linear structure (see Figure 4). The $\text{O}-\text{Ag}^+-\text{O}$ ADF shows a broad peak, indicating the variability of water ligand locations. The various peaks of it are certainly related to the existence of the aforementioned different ligand configurations varying with coordination numbers. The peak of the $\text{N}-\text{Ag}^+-\text{O}$ distribution centered at $\sim 90^\circ$ shows a relatively narrower range ($60\text{--}140^\circ$) compared to those of the $\text{N}-\text{Ag}^+-\text{N}$ and $\text{O}-\text{Ag}^+-\text{O}$ ADFs, indicating that, not with steady all conformational flexibility, NH_3 ligands are usually neighbored by water ligands.

To illustrate the instability of the first solvation shell, we have created a video clip available for download at the MOLVISION

TABLE 3: Characteristic Values for the Dynamics of Solvated Ag^+ in Aqueous Ammonia Solution

parameter	solvation shell	
	ammonia	water
$Q_{\text{Ag}^+-\text{L}}^a$	203, 223 (186) ^b	76, 119, 168 (99, 142, 186) ^b
MRT ^c	na ^d	1.1 (5.5) ^e
$N_{\text{ex}}^{0.5}/10$ ps	na	25 (11)
S_{ex}	na	0.36 (0.26)
$1/S_{\text{ex}}$	na	2.8 (3.8)

^a Ion-ligand stretching frequency in cm^{-1} . ^b Ion-ligand stretching frequency in cm^{-1} in the pure solvent.^{10,11} ^c Mean residence times in picoseconds. ^d No exchange observed within 13 ps; thus na = not applicable. ^e Data in the braces are obtained from the QM/MM MD simulation of the first hydration shell of Ag^+ in pure solvent.³⁴

homepage (<http://www.movision.com>, section video clips),³⁶ that shows the dynamics of solvent molecules in the surrounding Ag^+ . The solvated Ag^+ structures presented in Figure 4 were obtained by taking “snapshots” during the simulation.

3.2. Dynamical Data. The power spectrum of the Ag^+-N and Ag^+-O vibrational frequency observed for the solvation shell are displayed in Figure 5. A splitted peak located at 203 and 223 cm^{-1} was observed for the Ag^+-N vibrational frequency in the solvation shell caused by the asymmetry induced by the neighboring water dipoles. The corresponding force constants are 30 and 36 Nm^{-1} , showing higher values compared to that observed in liquid ammonia (26 Nm^{-1})¹¹ and, thus, indicate a stabilization of the ammonia ligands in the mixture. The peaks of the Ag^+-O vibrational frequency located at 76, 119, and 168 cm^{-1} correspond to force constants of 5, 12, and 23 Nm^{-1} , respectively, indicating the presence of three different types of bound by water ligands in the first solvation shell. The lower force constants compared to the Ag^+-N force constants reflect the high ligand flexibility due to very weak bonding.

The dynamical parameters of Ag^+ solvated in 18.6% aqueous ammonia solution are listed in Table 3. The extremely short mean residence time of 1.1 ps observed for water molecules in the solvation shell is less than the one obtained from the QM/

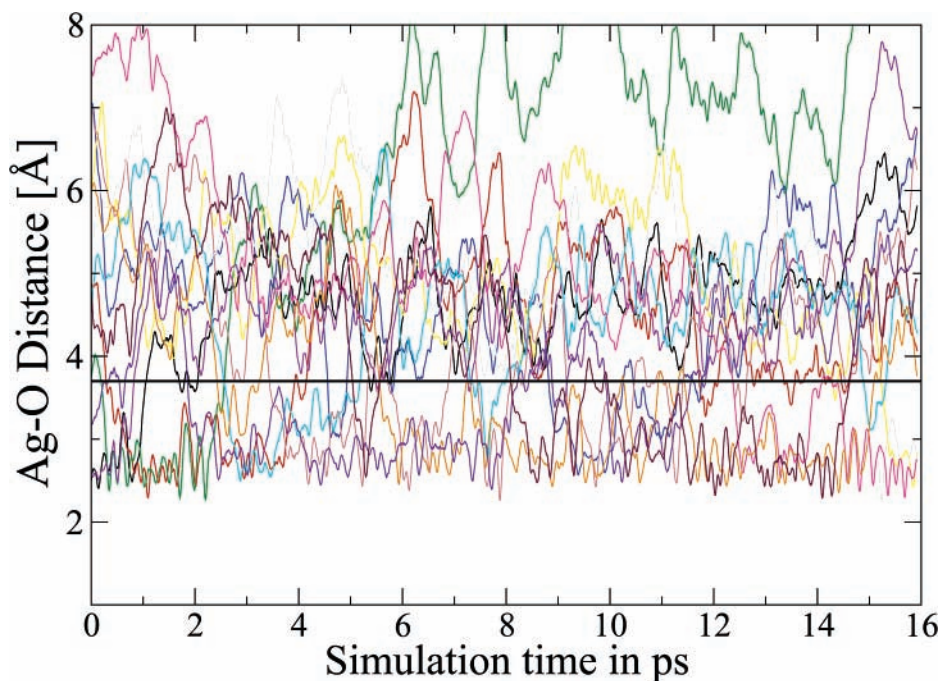


Figure 6. Distance plots of all water molecules participating at water-ligand exchange processes in the solvation shell within the simulation time of 13 ps.

MM simulation of Ag⁺ in water, pointing out that the binding of a few ammonia molecules can accelerate the exchange rate of water ligands at an ion as observed for hydrated Cu²⁺ amine complexes.^{37,38} This rapid water exchange (see Figure 6) could make water molecules in solvated Ag⁺ undetectable for XRD measurements,⁷ which obtained the Ag(NH₃)₂⁺ complex without a water ligand. The number of attempts needed for a persisting exchange, ($1/S_{\text{ex}}$) for water, is slightly lower than that obtained for Ag⁺ in water³⁴ (see Table 3), confirming that the formation of the ammonia complex increases the lability of water ligands in the ion's coordination shell. This lability is even higher than in the first hydration shell of Cs⁺³⁹ and, thus, indicates a remarkable structure breaking effect of the silver diamine complex for the surrounding solvent.

4. Conclusion

The QM/MM simulation technique has supplied many details of structural and dynamical properties of Au⁺ solvated in 18.6% aqueous ammonia solution. Three different complexes are predicted to be present in the solvation shell, namely [Ag(NH₃)₂(H₂O)₂]⁺, [Ag(NH₃)₂(H₂O)₃]⁺, and [Ag(NH₃)₂(H₂O)₄]⁺. The extremely short mean residence time of water ligands (1.1 ps) and the low force constant of the Ag⁺–O vibration reflect the high flexibility of water ligands, leading to a structure breaking effect in the surrounding solvent rather than to the formation of a second solvation shell.

Acknowledgment. Financial support for this work by the Austrian Science Foundation (FWF) (project P16221-N08) and a scholarship of the Austrian Federal Ministry for Foreign Affairs for R.A. are gratefully acknowledged.

References and Notes

- (1) Gabriel, M. M.; Mayo, M. S.; May, L. L.; Simmons, R. B.; Ahearn, D. G. *Curr. Microbiol.* **1996**, *33*, 1.
- (2) Nomiya, K.; Takahashi, S.; Noguchi, R.; Nemoto, S. *Inorg. Chem.* **2000**, *39*, 3301.
- (3) Shoeib, T.; Hopkinson, A. C.; Siu, K. W. M. *J. Phys. Chem. B* **2001**, *105*, 12399.
- (4) Boutreau, L.; Léon, E.; Rodríguez-Santiago, L.; Toulhoat, P. *J. Phys. Chem. A* **2002**, *106*, 9359.
- (5) Tsutsui, Y.; Sugimoto, K.; Wasada, H.; Funahashi, Y. I. S. *J. Phys. Chem. A* **1997**, *101*, 2900.
- (6) Yamaguchi, T.; Lindqvist, O. *Acta Chem. Scand.* **1983**, *A37*, 685.
- (7) Maeda, M.; Maegawa, Y.; Yamaguchi, T.; Ohtaki, H. *Bull. Chem. Soc. Jpn.* **1979**, *52*, 2545.
- (8) Bjerrum, J. *Acta Chem. Scand.* **1986**, *A40*, 392.

- (9) Yamaguchi, T.; Wakita, H.; Nomura, M. *J. Chem. Soc., Chem. Commun.* **1988**, 433.
- (10) Armunanto, R.; Schwenk, C. F.; Rode, B. M. *J. Phys. Chem. A* **2003**, *107*, 3132.
- (11) Armunanto, R.; Schwenk, C. F.; Randolph, B. R.; Rode, B. M. *Chem. Phys. Lett.* **2004**, *388*, 395.
- (12) Tongraar, A.; Rode, B. M. *J. Phys. Chem. A* **1999**, *103*, 8524.
- (13) Tongraar, A.; Sagarik, K.; Rode, B. M. *J. Phys. Chem. B* **2001**, *105*, 10559.
- (14) Tongraar, A.; Rode, B. M. *J. Phys. Chem. A* **2001**, *105*, 506.
- (15) Tongraar, A.; Sagarik, K.; Rode, B. M. *Phys. Chem. Chem. Phys.* **2002**, *4*, 628.
- (16) Schwenk, C. F.; Rode, B. M. *Phys. Chem. Chem. Phys.* **2003**, *5*, 3418.
- (17) Tongraar, A.; Liedl, K. R.; Rode, B. M. *J. Phys. Chem. A* **1997**, *101*, 6299.
- (18) Antolovich, M.; Lindoy, L. F.; Reimers, J. R. *J. Phys. Chem. A* **2004**, *108*, 8434.
- (19) Inada, Y.; Loeffler, H. H.; Rode, B. M. *Chem. Phys. Lett.* **2002**, *358*, 449.
- (20) Inada, Y.; Mohammed, A. M.; Loeffler, H. H.; Rode, B. M. *J. Phys. Chem. A* **2002**, *106*, 6783.
- (21) Schwenk, C. F.; Loeffler, H. H.; Rode, B. M. *J. Am. Chem. Soc.* **2003**, *125*, 1618–1624.
- (22) Schwenk, C. F.; Loeffler, H. H.; Rode, B. M. *J. Chem. Phys.* **2001**, *115*, 1080.
- (23) Schwenk, C. F.; Loeffler, H. H.; Rode, B. M. *Chem. Phys. Lett.* **2001**, *349*, 99.
- (24) Dunning, T. R. *J. Chem. Phys.* **1970**, *53*, 2823.
- (25) Hay, P. J.; Wadt, W. R. *J. Chem. Phys.* **1985**, *82*, 270.
- (26) Hannongbua, S. V.; Ishida, T.; Sphor, E.; Heizinger, K. Z. *Naturforsch., A: Phys. Sci.* **1988**, *43*, 572.
- (27) Kuchitsu, K.; Morino, T.; Maeda, M. *Bull. Chem. Soc. Jpn.* **1976**, *49*, 701.
- (28) Allen, M. P.; Tildesley, D. J. *Computer Simulation of Liquids*; Oxford University Press: Oxford, 1987.
- (29) Berendsen, H. J.; Grigera, J. R.; Straatsma, T. P. *J. Phys. Chem.* **1983**, *91*, 6269.
- (30) Bopp, P.; Jansc6, G.; Heinzinger, K. *Chem. Phys. Lett.* **1983**, *98*, 129.
- (31) Adams, D. J.; Adams, E. M.; Hills, G. J. *J. Mol. Phys.* **1985**, *38*, 387.
- (32) Markham, G. D.; Bock, J. P. G. C. L.; Trachtman, M.; Bock, C. W. *J. Phys. Chem.* **1996**, *100*, 3488.
- (33) Bopp, P. *Chem. Phys.* **1986**, *106*, 205.
- (34) Hofer, T. S.; Tran, H. T.; Schwenk, C. F.; Rode, B. M. *J. Comput. Chem.* **2004**, *25*, 211.
- (35) Seward, T. M.; Henderson, C. M. B.; Charnock, J. M.; Dobson, B. R. *Geochim. Cosmochim. Acta* **1996**, *60*, 2273.
- (36) Tran, H. T.; Rode, B. M. <http://www.molvision.com> (accessed 2002).
- (37) Sandstr6m, M.; Neilson, G. W.; Johansson, G.; Yamaguchi, T. *J. Phys. C: Solid State Phys.* **1985**, *18*, L1115.
- (38) Schwenk, C. F.; Rode, B. M. *Phys. Chem. Chem. Phys.* **2003**, *5*, 3418–3427.
- (39) Schwenk, C. F.; Hofer, T. S.; Rode, B. M. *J. Phys. Chem. A* **2004**, *108*, 1509.